Analysis of Plastic Flow Instability During Superplastic Deformation of the Zn-Al Eutectoid Alloy Modified with 2 wt.% Cu

Mitsuo Ramos-Azpeitia, E. Elizabeth Martínez-Flores, JoseLuis Hernandez-Rivera, and Gabriel Torres-Villaseñor

The aim of this work is to analyze the plastic flow instability in Zn-21Al-2Cu alloy deformed under 10^{-3} s^{-1} and 513 K, which are optimum conditions for inducing superplastic behavior in this alloy. An evaluation using the Hart and Wilkinson–Caceres criteria showed that the limited stability of plastic flow observed in this alloy is related to low values of the strain-rate sensitivity index (m) and the strain-hardening coefficient (γ), combined with the tendency of these parameters to decrease depending on true strain (ε). The reduction in m and γ values could be associated with the early onset of plastic instability and with microstructural changes observed as function of the strain. Grain growth induced by deformation seems to be important during the first stage of deformation of this alloy. However, when $\varepsilon > 0.4$ this growth is accompanied by other microstructural rearrangements. These results suggest that in this alloy, a grain boundary sliding mechanism acts to allow a steady superplastic flow only for $\varepsilon < 0.4$. For ε values between 0.4 and 0.7, observed occurrences of microstructural changes and severe neck formation lead to the supposition that there is a transition in the deformation mechanism. These changes are more evident when $\varepsilon > 0.7$ as another mechanism is thought to take over.

1. Introduction

Superplasticity is the ability of a polycrystalline material to exhibit high tensile elongations. The stable nature of superplastic deformation is important for the commercial application of materials that exhibit this behavior. During superplastic deformation, plastic flow stability is maintained until neck onset. When the neck is formed, it progresses diffusely, allowing a greater elongation because it has a very high localized necking resistance. This resistance is a consequence of the high sensitivity to strain rate (m) (Ref 1-3). Experimentally, it has been observed that during superplastic deformation, several diffuse necks form and soften (Ref 4). This process continues until the growth of any one neck begins to dominate and accelerate, causing a localized plastic deformation. Therefore, plastic flow instability is dependent on the true strain (ε), which causes the material to fracture (Ref 4-6).

Mitsuo Ramos-Azpeitia and **E. Elizabeth Martínez-Flores**, Facultad de Ingeniería, Universidad Autónoma de San Luis Potosí, Dr. Manuel Nava 8, Zona Universitaria, 78290 San Luis Potosí, SLP, Mexico; **Jose Luis Hernandez-Rivera**, CONACYT-Instituto de Metalurgia, Universidad Autónoma de San Luis Potosí, Sierra Leona 550, Lomas 2ª Sección, 78210 San Luis Potosí, SLP, Mexico; and **Gabriel Torres-Villaseñor**, Instituto de Investigación en Materiales, UNAM, P. O BOX 70-360, 04519 Mexico, DF, Mexico. Contact e-mail: mitsuo.ramos@uaslp.mx.

The instability of superplastic deformation has been the subject of several studies (Ref 5-9). Hart developed a tensile stability criterion for materials that exhibit both strain hardening and strain-rate hardening (Ref 5). In this criterion, it is proposed that deformation is stable if the magnitude of the cross-sectional difference does not increase as deformation progresses. Hart's criterion is defined as:

$$\gamma + m \geq 1 \qquad \text{(Eq 1)}$$

For this criterion, the strain-hardening coefficient (γ) and the strain-rate sensitivity index (m) can be expressed by the following equations:

$$\gamma = \frac{1}{\sigma}\left(\frac{\partial \sigma}{\partial \varepsilon}\right) \qquad \text{(Eq 2)}$$

$$m = \frac{\dot{\varepsilon}}{\sigma}\left(\frac{\partial \sigma}{\partial \dot{\varepsilon}}\right) \qquad \text{(Eq 3)}$$

In addition to Hart´s stability criterion, Wilkinson and Caceres proposed an instability parameter (I) to describe the development of instability under uniaxial tension (Ref 7). In this criterion, the onset of plastic instability can be studied by evaluating parameter I, defined as (Ref 8, 9):

$$I = \frac{1 - \gamma - m}{m} \qquad \text{(Eq 4)}$$

This parameter indicates that the onset of plastic instability occurs when $I = 0$, which is equivalent to Hart's stability criterion ($\gamma + m = 1$). The value of I indicates how fast the plastic instability advances, since the greater the value of I, the more unstable the deformation is and localized necking occurs. Therefore, to achieve plastic stability $I < 1$ is needed. In order to

evaluate this parameter, it is necessary to calculate the value of the strain-hardening coefficient (γ) using the following expression, which is valid when grain growth increases linearly with the strain (ε) (Ref [7], [8]):

$$\gamma = \frac{Cpm}{d_0 + C\varepsilon} \qquad \text{(Eq 5)}$$

In this equation, p is the grain size sensitivity, d_o is the initial grain size and C is a constant representing the value of the slope in a plot of grain size growth ($\Delta d = d - d_o$) as a function of ε when tests are performed at constant strain rate ($\dot{\varepsilon}$) and temperature.

Furthermore, stable plastic flow during superplastic deformation is obtained when the mechanism that acts to achieve steady flow conditions remains constant with increasing strain. A high value of strain-rate sensitivity is associated with the grain boundary sliding (GBS) mechanism, which has been reported as the dominant deformation process in superplastic materials such as Zn-Al eutectoid alloy (Ref [10-12]). Therefore, evaluation of plastic stability in this alloy can provide information regarding possible changes in deformation mechanism when alloying elements are added to improve its mechanical properties.

The Zn-21Al-2Cu alloy is a modified Zn-Al eutectoid alloy that has shown superplastic behavior, reaching a maximum strain of about 1000% (Ref [13]). In this paper, the analysis of plastic flow instability is performed under optimal conditions of superplastic deformation as a function of true strain. This work aims to investigate the role of 2 wt.%. Cu addition on the plastic stability of a Zn-Al eutectoid alloy by evaluating the Hart and Wilkinson–Caceres criteria parameters. The values of these parameters will be related to changes observed in the microstructure of the superplastically deformed Zn-22Al-2Cu alloy. These values may be evidence of changes in the deformation mechanism acting upon this alloy.

2. Experimental Procedure

The Zn-21Al-2Cu alloy was prepared by melting Zn, Al and Cu of high purity (99.99%) in an induction furnace. A 38-mm-diameter rod was obtained by continuous casting. This rod was cut, hot-extruded at 563 K (Extrusion Relation = 11) and hot-rolled at 513 K to obtain sheets of 2.54 mm thickness. Specimens with a gauge length (L_0) of 6.35 mm for tensile testing were machined from the rolled sheets. After machining, the specimens were solution treated at 623 K for 1 h. Then, they were quenched in ice water at 288 K and annealed at 533 K for 20 min. After this heat treatment, all specimens attained a fine-grained microstructure with an average grain size of 0.85 ± 0.065 μm. This microstructure consists of a fine and homogeneous mixture of 0.492 and 0.489 by volume fraction of α and η, which are Al- and Zn-rich phases, respectively. Additionally, grain phase measurements performed on the initial fine microstructure obtained a grain size of 0.88 ± 0.058 μm for α and 1.04 ± 0.060 μm for η. All grain measurements were performed by the intercept method and were consistent with previous measurements performed on the same alloy with similar heat treatment using the electron backscatter diffraction (EBSD) technique (Ref [14]). Clusters of fine grains of τ' phase (Al_4Cu_3Zn), which represent a volume fraction of 0.019, were also observed in the initial microstruc-

ture. All volume fraction determination was performed by the Rietveld refinement analyses of XRD patters using the MAUD program. Before testing, specimens were polished with fine diamond pastes to achieve a mirror-like surface.

In order to study the flow localization of the Zn-21Al-2Cu alloy, tensile tests were performed at constant crosshead speed in a Shimadzu AG-I Universal Testing Machine equipped with a thermal chamber. Specimens were deformed at 513 K and initial strain rates ($\dot{\varepsilon}$) of 10^{-3} s^{-1} (optimal superplastic conditions). Tensile tests were performed to achieve the following engineering strain values ($e = \Delta L/Lo$): 15, 30, 50, 75, 100, 150, 200 and 300%. The method proposed by Mohamed and Langdon (Ref [15]) was used to characterize the localization and uniformity of the plastic flow. In this method, the gauge length (Lo = 6.35 mm) of each specimen is carefully etched with a series of parallel lines to divide it into sections of equal length (lo). For this study, each specimen was divided into seven sections with a width of about 0.9 mm, as shown in Fig. 1.

The localization of the plastic flow was determined by calculating the deformation of each section as $\Delta l/lo$, where Δl is the increase in the length of each small segment. The uniformity of the plastic flow is evaluated by plotting the maximum ($\Delta l/lo$) and minimum ($\Delta l/lo$) against ($\Delta L/Lo$). Finally, microstructural changes on the surface of deformed specimens were characterized using a Philips XL-30 scanning electron microscope.

3. Results

3.1 Localization and Uniformity of the Plastic Flow in Optimal Superplastic Conditions

The tensile-deformed specimens, at fixed engineering strain values (e), are shown in Fig. 2. It can be noted that plastic deformation is stable up to values of about 100%. For specimens tensile deformed more than 100%, the presence of two types of necks along the gauge length—a sharp-shaped neck in adjacent gripping areas and a more diffuse neck around the central part—is evidence of plastic instability onset.

The tensile specimens that are shown in Fig. 2 present a localized and non-uniform plastic flow. These aspects were evaluated by using the method proposed by Mohamed and Langdon (Ref [15]), and results are presented in Fig. 3(a) and (b). The graphs in Fig. 3(a) illustrate that the deformation is quasi-uniform throughout gauge length when $\Delta L/Lo \leq 50\%$. For $\Delta L/Lo$ values between 50 and 150%, plastic flow begins to be greater in Sects. 5 and 6, as shown in Fig. 1. For $\Delta L/Lo > 150\%$, plastic flow localization is also more evident in these sections.
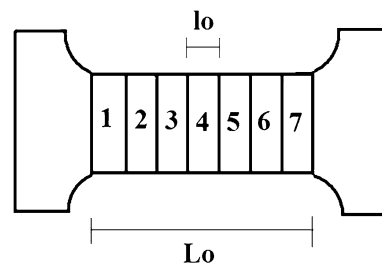
Fig. 1 Schematic illustration of the specimen gauge length Lo, showing the division into seven segments, each of length lo
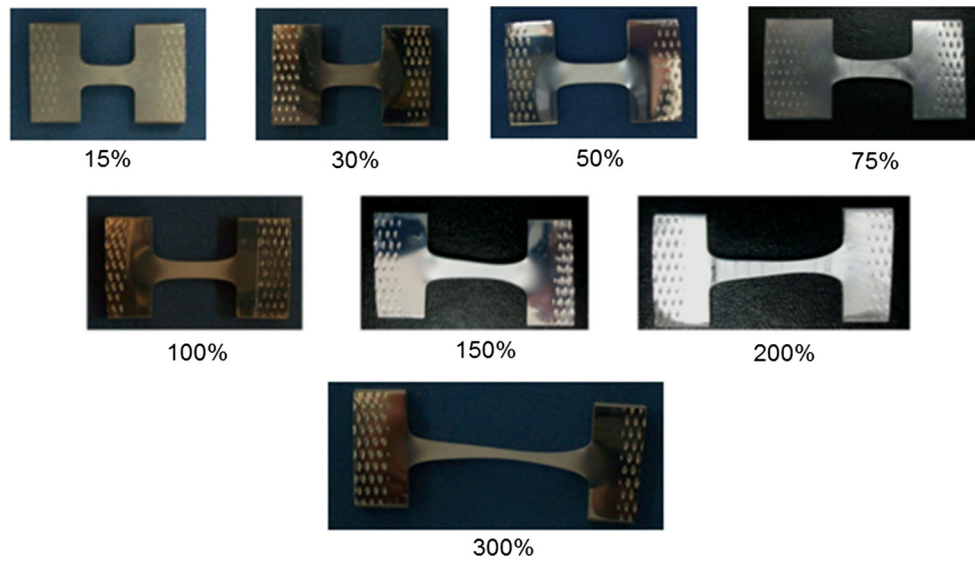
Fig. 2 Zn-21Al-2Cu alloy tensile specimens, to different fixed engineering strains values, tested at 10^{-3} s^{-1} and 533 K

(a)

(b)
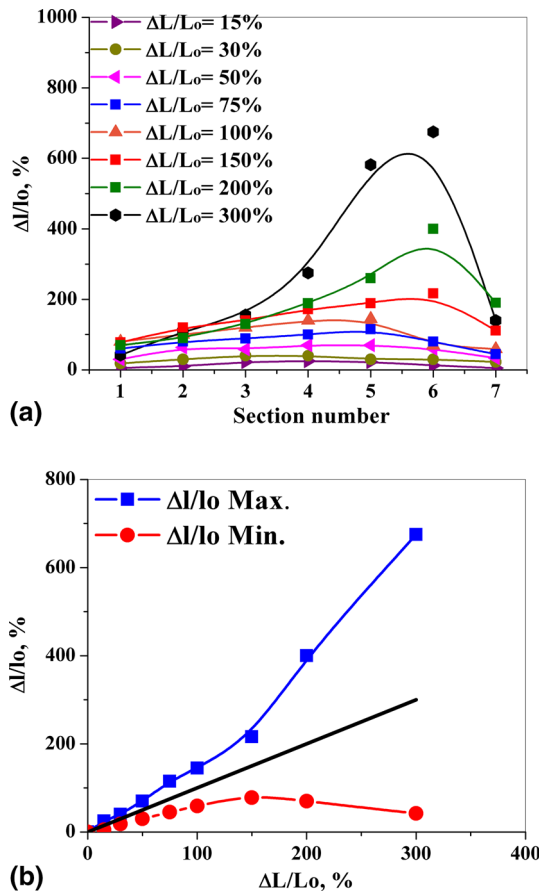
Fig. 3 (a) Plot of $\Delta l/l_o$ vs. section number to evaluate the localization of plastic flow in Zn-21Al-2Cu alloy. (b) Plot $\Delta l/l_o$ minimum vs. $\Delta l_o/l_o$ maximum to evaluate the uniformity level of plastic flow in Zn-21Al-2Cu alloy (solid black line represents the ideal uniformity)

When $\Delta L/L_o$ reaches 300%, all deformation is localized almost entirely within these two segments. This is consistent with the tensile-deformed specimens shown in Fig. 2.

The results shown in Fig. 3(a) give information about plastic flow localization but do not provide quantification of the strain uniformity. If the plastic flow is totally uniform, then the deformation of each gauge length section should be the same as the total deformation, i.e., $\Delta l/l_o = \Delta L/L_o$. This situation is represented by a solid black line in Fig. 3(b), which also shows values for $\Delta l/l_o$ minimum and maximum obtained from the data in Fig. 3(a). The analysis of the results in Fig. 3(b) provides a quantification of the plastic flow uniformity level and confirms that the deformation remains uniform up to $\Delta L/L_o = 50\%$. For elongations up to $\Delta L/L_o = 100\%$, the uniformity begins to decrease gradually. For elongations $\Delta L/L_o > 100\%$, there is a marked deviation from uniform behavior.

3.2 Plastic Instability Analysis

Evaluation of plastic flow instability in Zn-21Al-2Cu alloy was performed on specimens tensile deformed under superplastic optimal conditions ($\dot{\varepsilon} = 10^{-3}$ s^{-1} and $T = 513$ K), using both Hart (Ref 5) and Wilkinson–Caceres criteria (Ref 7). In the Hart criterion, the m and γ values are considered constant, while the Wilkinson–Caceres criterion proposes that γ varies due to grain growth, which occurs during deformation. In a previous work, where superplastic behavior of Zn-21Al-2Cu alloy was analyzed in optimal conditions, evidence of microstructural changes after superplastic deformation was found (Ref 13). Taking into account these observations, in the current investigation the estimation of m and p values was made by considering their change as a function of true strain. The values for these estimations were obtained using the method proposed by Rao and Mukherjee (Ref 16). To obtain the m parameter values, log σ against log $\dot{\varepsilon}$ plots for different values of ε were constructed using data of tensile tests carried out at 513 K and strain-rate values of 5×10^{-4}, 1×10^{-3}, 2×10^{-3} and 5×10^{-3} s^{-1} (Fig. 4a). The value of m as a function of ε can be estimated from slope values in log σ against log $\dot{\varepsilon}$ plots.

In order to estimate p values, log σ against log d plots for distinct values of ε were constructed using data corresponding to tensile tests carried out at 10^{-3} s^{-1} and 513 K in specimens with an initial grain size of 0.85, 2.05 and 4.5 μm (Fig. 4b).
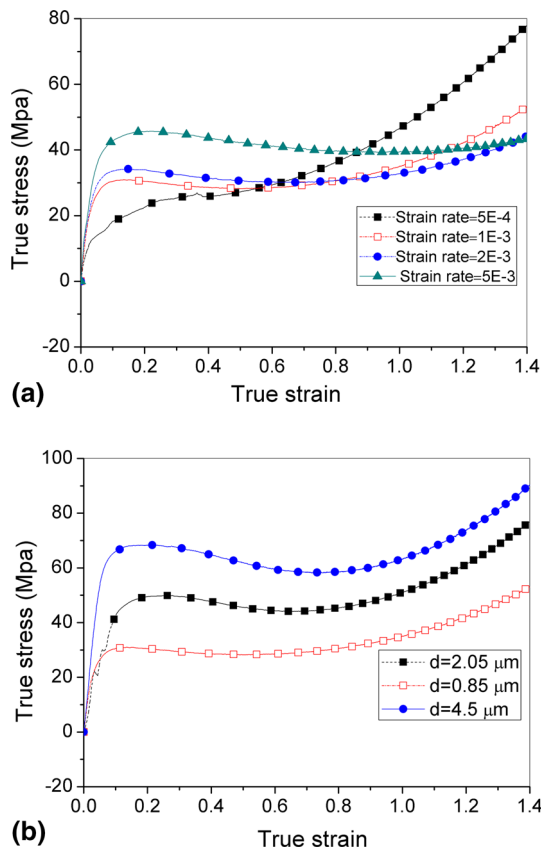
Fig. 4 (a) Plots of log σ against log ε at $T = 513$ K for Zn-21Al-2Cu alloy superplastically deformed at different strain-rate values. (b) Plots of log σ against log ε at $T = 513$ K for Zn-21Al-2Cu alloy superplastically deformed at different initial grain sizes values

Fig. 5 (a) Values of m parameter estimated as function of true strain for Zn-21Al-2Cu alloy superplastically deformed at 533 K. (b) Values of p parameter estimated as function of true strain for Zn-21Al-2Cu alloy superplastically deformed at 533 K
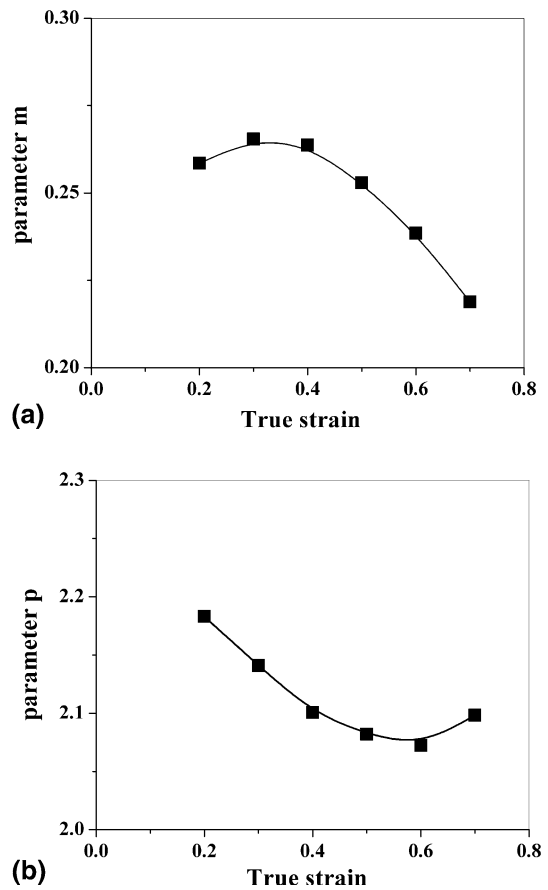
Values for p were estimated as a function of ε from the slope values in the plots and values for parameter n, calculated using the relationship $n = 1/m$, with the expression:

$$p = n \frac{\partial \log \sigma}{\partial \log d} \qquad \text{(Eq 6)}$$

The values of m and p were estimated only for ε between 0.2 and 0.7 because for longer true strain, the value of σ becomes invalid due to the flow localization observed in Fig. 2.

The m and p parameter values as a function of ε are shown in Fig. 5(a) and (b), respectively. The m value decreased after it achieved a maximum of 0.26 at $\varepsilon = 0.3$, while for p, a maximum value of 2.18 is obtained when $\varepsilon = 0.2$, before reaching a minimum at $\varepsilon = 0.6$. Similar behavior for the values of the m and p parameters as a function of true strain was reported for a superplastic 7075 Al alloy and was related to microstructural changes (Ref 16). For 7075 alloy, m values decrease from 0.8 down to a steady value of 0.5 and p values change from 2.16 to 1.26. In particular, large magnitude changes in parameter p were associated with a dislocation activity occurring within the grain interior, leading to grain elongation. After comparing the results for both alloys, it can be assumed that in the Zn-21Al-2Cu alloy microstructural changes occur during deformation leading to a drop in m and p parameters.

Grain growth after superplastic deformation, which increases in magnitude with strain, has been reported in different

alloys (Ref 7, 9). This grain growth induced by strain produces an effective strain hardening which affects the γ value (Ref 7). Therefore, in order to obtain an estimation of the γ parameter as a function of strain, it is first necessary to determine quantitatively the contribution of the strain to grain growth. The procedure is performed by plotting Δd against ε, where Δd values correspond to the difference between grain size measurements in deformed specimens and initial grain size (d_o). In Fig. 6(a), the results of this determination for the Zn-21Al-2Cu alloy are shown. The grain size measurements, which were taken using the intercept method, were carried out in deformed specimens after ε values of 0.14, 0.26, 0.40, 0.56 and 0.69. These measurements are in accordance with previous results obtained for the same alloy using the electron backscatter diffraction (EBSD) technique (Ref 14). The results in Fig. 6(a) show the occurrence of a strain-dependent grain growth during superplastic deformation, which increases in a linear manner with strain. In this plot, the slope value represents the value of constant C from Eq 5. For the Zn-21Al-2Cu alloy, the value observed was 1.13. Similar behavior reported for the Zn-22Al-0.5Cu alloy is schematized in the figure for comparison.

The values of p, m and constant C were replaced in Eq 5 in order to estimate the strain-hardening coefficient (γ) as a function of true strain (ε). Figure 6(b) shows that the γ value reaches a maximum of 0.75 at $\varepsilon = 0.3$, and then, it decreases to 0.60 for $\varepsilon = 0.7$. This behavior is associated with a deformation
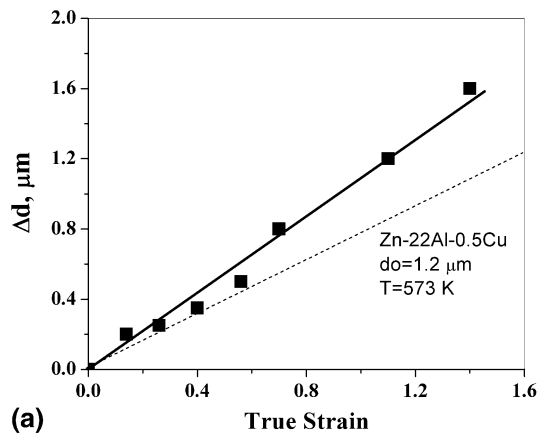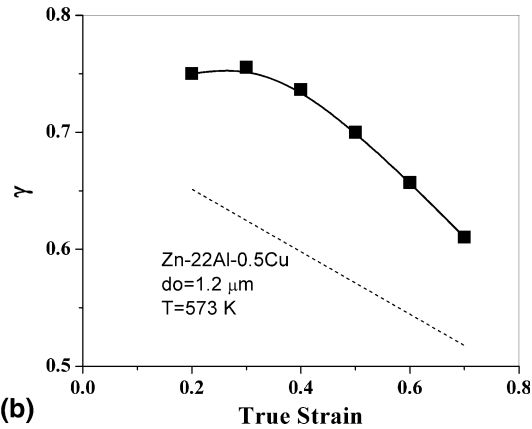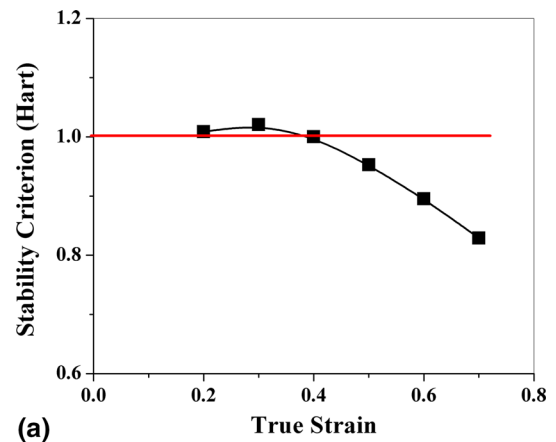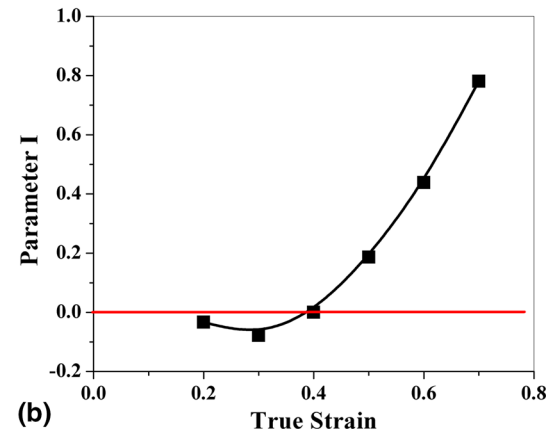
Fig. 6 (a) Grain size increment as a function of true strain for the calculation of constant *C*. (b) Estimation of the strain-hardening coefficient *γ* as function of the true strain for the Zn-21Al-2Cu alloy superplastically deformed in optimal conditions


Fig. 7 (a) Evaluation of the stability criterion proposed by Hart as function of the true strain increase for the Zn-21Al-2Cu alloy superplastically deformed at *T* = 513 K. (b) Evaluation of the instability parameter proposed by Wilkinson and Caceres as function of the true strain increase for the Zn-21Al-2Cu alloy superplastically deformed at *T* = 513 K

hardening effect whose magnitude decreases for $\varepsilon > 0.3$. These findings are similar to those reported by Wilkinson and Caceres for the Zn-22Al-0.5Cu alloy (Ref 17). However, in that particular case, values for *γ* fall from 0.69 to 0.53 for the same true strain range, as can be observed in Fig. 6(b), where results for the Zn-22Al-0.5Cu alloy are schematized. The fall in the *γ* values is quantitatively similar in both alloys, nevertheless, *γ* values are greater in the Zn-21Al-2Cu alloy as consequence of its higher Cu content.

The evaluation of the stability criterion proposed by Hart (Ref 5) for Zn-22Al-2Cu alloy, which is shown in Fig. 7(a), was carried out using the previously estimated *m* and *γ* values. From this figure—where the critical value for instability onset is indicated by a horizontal line—it can be observed that plastic instability begins at $\varepsilon = 0.4$. On the other hand, using the previously estimated values of *C*, *m* and *γ*, it was possible to evaluate the plastic instability parameter (I) proposed by Wilkinson and Caceres using Eq 4 (Ref 8). The result of this evaluation, which is shown in Fig. 7(b), confirms that plastic instability onset occurs at $\varepsilon = 0.4$ and shows that this inhomogeneous flow grows suddenly for large true strains. These findings are in accordance with the deformation sequence observed in the tensile specimens of Fig. 2, where the plastic instability begins at tensile strains greater than 50% ($\varepsilon > 0.4$), in addition to the evaluation of the plastic flow localization and uniformity shown in Fig. 3. The stability

criterion evaluation for the Zn-21Al-2Cu alloy revealed important differences as compared to the Zn-22Al-0.5Cu alloy that, under similar superplastic deformation conditions, exhibits plastic instability onset according to the *I* parameter beginning at $\varepsilon = 1.0$ and progressing in a quasi-stable way until values approach $\varepsilon = 3.5$ (Ref 17).

3.3 Microstructural Characterization as a Function of Strain

The plastic flow in steady state for Zn-21Al-2Cu alloy prevails up to a strain value of 0.4, while for large true strains plastic flow begins to become unstable, as explained in the previous section. In a previous work, the presence of an unstable plastic flow and microstructural changes, consisting of aligned grains of the *η* phase (Zn-rich phase) following maximum engineering elongation in this alloy after superplastic deformation under optimal conditions was reported (Ref 13). These microstructural changes can be related to the decrease in *m* and *γ* values as a function of true strain as was determined in this work.

In order to examine whether these microstructural changes can be a function of increasing strain, a surface analysis using SEM was carried out in the middle part of samples tensile deformed up to true strain (ε) values of 0.14, 0.40, 0.69 and
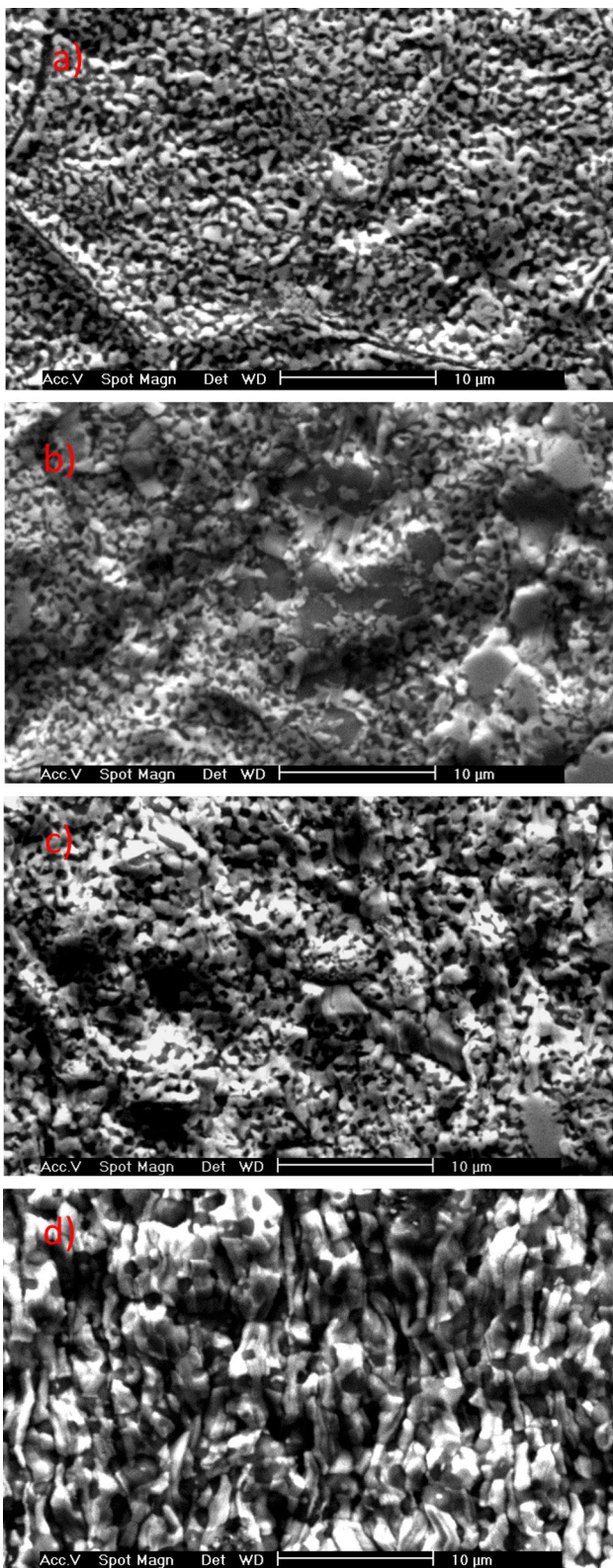
Fig. 8 SEM micrographs corresponding to different fixing true strain values, showing microstructural changes as consequence of the deformation in Zn-21Al-2Cu alloy deformed at 513 K and 1×10^{-3} s^{-1}: (a) $e = 0.14$, (b) $e = 0.40$, (c) $e = 0.69$ and (d) $e = 1.38$. All SEM micrographs at 3000X

1.38, respectively. Corresponding micrographs at 3000X are shown in Fig. 8. After $\varepsilon = 0.14$ (Fig. 8a), the microstructure consists of a mixture of fine and equiaxed α and η grains, which are an Al-rich phase (dark phase) and Zn-rich phase (bright phase), respectively. For $\varepsilon = 0.40$, the fine, equiaxed microstructure is accompanied by zones of α and η phases with increased sizes, which was revealed to be a consequence of the deformation (Fig. 8b). In Fig. 8(c), for a true strain of 0.69, grain growth of both α and η phases is observed, while η grains show a tendency to be aligned along the tensile direction. In Fig. 8(d), flow bands aligned in the tensile direction and an increased grain growth in α and η fine phases were observed for a true strain of 1.38. These microstructural features correspond to those previously reported in a specimen tensile deformed up to fracture strain of 1000% for this alloy under the same experimental conditions (Ref 13).

4. Discussion

In a previous work, it was suggested that in the Zn-21Al-2Cu alloy deformed at conditions that allow maximum attainable elongation ($\dot{\varepsilon} = 10^{-3}$ s^{-1} and $T = 513$ K), there are changes in the deformation mechanism, evidenced by the early presence of an inhomogeneous plastic flow (Ref 13). In the present investigation, a more detailed study of the plastic instability process for this alloy under such conditions was carried out in order to obtain additional information which supports that proposal and helps to elucidate the role of Cu additions as high as 2 wt.% in the superplastic stability of a Zn-22Al eutectoid alloy.

The flow localization and uniformity of the neck formation process for this alloy were evaluated in the first part of this study (Fig. 3). The results show the presence of a flow localization which begins at $e = 50\%$ and continues in a quasi-stable manner up to $e = 100\%$, before finally exhibiting a marked deviation from uniformity at large strains. This behavior is different from that reported for the Zn-22Al alloy, wherein a very stable plastic flow is maintained up to strain values close to 350% and then quasi-stable up to values of 770% under similar experimental conditions (Ref 15). The current results show that the addition of 2 wt.% Cu in Zn-22Al alloy decreases plastic flow stability when the deformation is carried out under optimal superplastic conditions (region II) by a factor of seven. However, the current results are congruent with those reported for region I of a Zn-22Al alloy where the early appearance of an inhomogeneous flow is directly related to a decrease in m values from 0.45 to 0.25 (Ref 15). Therefore, the addition of at least 2 wt.% of Cu has an important role in decreasing the strain-rate sensitivity of this alloy and, as a consequence, its plastic stability. This result complements past investigations on the role of Cu in Zn-22Al alloy, in which it was concluded that additions up to 1 wt.% of Cu do not have a significant effect on the superplastic forming behavior of this alloy (Ref 18).

The analysis of plastic instability accomplished in the second part of this study included the estimation of m and γ parameters as a function of the true strain (ε). The neck growth depends on the capacity of the parameter m to remain stable, according to the relationship (Ref 15):

$$\frac{-\mathrm{d}A}{\mathrm{d}t} = \left(\frac{P}{B}\right)^{1/m} A^{(m-1)/m} \qquad \text{(Eq 7)}$$

where A is the cross-sectional area of the specimen, t is the time, $B = \sigma/\dot{\varepsilon}^m$ and P is the tensile force. A value of $m < 0.3$ is associated with microscopic neck formation within the gauge length (Ref 19, 20). The results shown in Fig. 3(a) are evidence that the superplastic deformation in Zn-21Al-2Cu alloy is carried out with an initial m value less than 0.3, and then, this value tends to decrease for $\varepsilon > 0.4$. In accordance with Eq 7, the low value of the m parameter estimated in this work ($m \approx 0.26$), and its tendency to decrease as function of true strain, does not allow conditions for a steady plastic flow to be maintained. This situation leads to the development of an inhomogeneous plastic flow, which progresses with the true strain, resulting in the formation of necks such as those observed in the corresponding specimens tensile deformed higher than 50% (Fig. 2). This affirmation is supported by the evaluation of both the Hart (Ref 5) and Wilkinson–Caceres (Ref 8) criteria in Fig. 7, which shows that the onset of plastic instability occurs at $\varepsilon = 0.4$ (50%).

In order to achieve a complete, uniform macroscopic deformation in the Zn-21Al-2Cu alloy, parameters m and γ must at least maintain their initial values. However, the results obtained in this study show that the plastic instability onset in this alloy is associated with low initial values of both parameters and their tendency to decrease as a function of ε. It is important to note that the method of evaluating the plastic stability with both the Hart and Wilkinson–Caceres criteria used in this work is more accurate because it considers changes in both m and γ parameters as a function of strain. Therefore, it is proposed that when microstructural changes are observed in superplastic alloys, it is convenient to consider the estimation of these parameters as a function of the true strain for the evaluation of plastic instability.

In Fig. 5, the values of m and p showed a tendency to decrease with increasing ε. This behavior influences the value of the strain-hardening coefficient (γ) as a function of ε according to Eq 5 and can be explained by the presence of microstructural changes, which occur gradually during the deformation process. These changes, observed in Fig. 8, can be involved in grain growth and the modification of shape and distribution of the phases in the microstructure. Particularly, the change in parameter p could be associated with a grain growth tendency. In Fig. 6(a), the results show that for this alloy, there exists a grain growth induced by deformation that is linearly dependent on the true strain. It is important to note that this evaluation considered both the static (diffusion-assisted) and the dynamic (deformation-assisted) contributions to the grain growth. An additional evaluation of each individual contribution showed that the static component only represented about 10% of the total grain growth; therefore, there is strong evidence that supports the idea that the principal role of Cu addition as high as 2 wt.%. is to facilitate the superplastic deformation-assisted grain growth in this alloy. This kind of linear dependence was also reported for the Zn-22Al alloy doped with 0.5 wt.% Cu, with the conclusion that the primary role of the Cu is to promote grain growth behavior (Ref 17). Considering the above results, in the Zn-22Al eutectoid alloy,

grain growth induced by deformation is two times greater with a Cu addition of 2 wt.%., than that observed with a Cu addition of 0.5 wt.%., when the superplastic deformation is carried out under the same conditions (Ref 17, 21).

From the initial microstructural characterization, it is possible to note that the grain growth behavior seems different between α and η phases. In particular, it was observed that the grain growth in η phase tends to be higher than that observed in α phase (see the series in Fig. 8). Generally, the grain growth during superplastic deformation is attributed to an increase in grain boundary mobility or in the driving force for grain boundary migration (Ref 22, 23), which can be different in each phase of duplex alloys (Ref 23). Previous studies in Zn-Al alloys also showed evidence of greater grain growth in the Zn-rich phase than in Al-rich phase (Ref 24, 25), which is in accordance with the observations made in the present work. The model for deformation-induced grain growth proposed by Wilkinson and Caceres (Ref 8) can explain the grain behavior observed in the present work. This model suggests that in micro-duplex materials, grain growth results from an enhanced coarsening of the second phase particles as they are brought into contact by grain switching during superplastic flow. If a model such as the one proposed by Wilkinson and Caceres acts during the superplastic deformation, then microstructural changes similar to those observed in Fig. 8 could be expected. This proposition is also supported by studies carried out in other alloys, which show that superplastic deformation leads to morphological and chemical changes by a process where the redistribution of elements by diffusion is significant (Ref 26). These kinds of movements by alloying elements have also been reported in other superplastic alloys (Ref 27). However, a more in-depth study that includes an analysis of the mobility and redistribution of the Zn, Al and Cu elements in the phases of the Zn-21Al-2Cu alloy and their relationship with the deformation-induced grain growth will be necessary. Additionally, a more thorough evaluation and characterization of the microstructural changes under several superplastic deformation conditions using several different characterization techniques are currently being carried out. The results obtained from this analysis will be reported in a future manuscript.

Finally, the occurrence of microstructural changes in the Zn-21Al-2Cu alloy that lead to a decrease in m and γ values began at true strains greater than 0.4. The decrease in these values indicates a tendency to inhibit the operation of a grain boundary sliding (GBS) mechanism as the strain increases. The above results suggest that in this alloy, a GBS mechanism brings on a stationary superplastic flow only for $\varepsilon < 0.4$. For true strains between 0.4 and 0.7, there is a transition stage for this mechanism, which is characterized by macro- and microstructural changes. The onset of microstructural changes is more evident for $\varepsilon > 0.7$, where another mechanism associated with low values of m could probably be acting. If the superplastic behavior of Zn-22Al eutectoid alloy free of Cu is compared with the corresponding behavior of Zn-21Al-2Cu alloy, it is evident that the addition of 2 wt.%. Cu promotes change in the GBS mechanism for true strains higher than 0.4. A follow-up study to determine the nature of the change in the GBS mechanism for this alloy and the specific role of the Cu is in progress.

5. Conclusions

The main conclusions that can be derived from this work are listed below:

1. The addition of 2 wt.% Cu to the eutectoid Zn-22Al alloy decreases the stable superplastic capacity of this alloy sevenfold.

2. In optimal conditions, the maximum strain attainable in the Zn-21Al-2Cu alloy is close to 1000%. However, superplastic deformation is stable only up to an engineering strain of 50% ($\varepsilon = 0.4$) and quasi-stable up to 100% ($\varepsilon = 0.7$). For greater strains, the deformation is highly localized.

3. The onset of plastic instability as determined by the Hart and Wilkinson–Caceres criteria occurs at $\varepsilon = 0.4$, which is consistent with the low initial values of the m and γ parameters and their tendency to decrease as a function of the true strain.

4. The decrease in the m and γ parameters can be related to the occurrence of microstructural changes during deformation. These changes can be involved in the deformation-induced grain growth in the α and η fine phases.

5. It was observed that the presence of 2 wt.%. Cu doubles the rate of deformation-induced grain growth compared to the Zn-22Al eutectoid alloy doped with 0.5 wt.% Cu. This grain growth seems to occur predominately in the Zn-rich phase.

6. For the Zn-21Al-2Cu alloy, the plastic instability onset is evidence that the GBS mechanism, which allows a superplastic flow in steady state, is dominant only in the first stage of the deformation process.

References

1. K.A. Padmanabhan, R.A. Vasin, and F.U. Enikeev, *Superplastic Flow: Phenomenology and Mechanics*, Springer, Berlin, 2001
2. D.M.R. Taplin, G.L. Dunlop, and T.G. Langdon, Flow and Failure of Superplastic Materials, *Annu. Rev. Mater. Sci.*, 1979, **9**, p 151–189
3. H.P. Stuwe and P. Les, Strain Rate Sensitivity of Flow Stress at Large Strains, *Acta Mater.*, 1998, **46**, p 6375–6380
4. G.E. Dieter, *Mechanical Metallurgy*, Mc Graw-Hill, Singapore, 1988, p 751
5. E.W. Hart, Theory of Tensile Test, *Acta Metall.*, 1967, **15**, p 351–355
6. J.W. Hutchinson and K.W. Neale, Influence of Strain-Rate Sensitivity on Necking Under Uniaxial Tension, *Acta Metall.*, 1977, **25**, p 839–846
7. D.S. Wilkinson and C.H. Caceres, On the Mechanism of Strain-Enhanced Grain-Growth During Superplastic Deformation, *Acta Metall.*, 1984, **32**, p 1335–1345
8. C.H. Caceres and D.S. Wilkinson, Large Strain Behavior of a Superplastic Copper Alloy—1. Deformation, *Acta Metall.*, 1984, **32**, p 415–422
9. D.S. Wilkinson, Microstructural instability during superplastic flow, in *Superplastic Forming of Structural Alloys: Proceedings of a Symposium*, N.E. Paton and C.H. Hamilton, Eds., Metallurgical Society of AIME, Warrendale, PA, 1982, p 81–89
10. T.G. Langdon, Grain Boundary Sliding Revisited: Developments in Sliding Over Four Decades, *J. Mater. Sci.*, 2006, **41**, p 597–609
11. A. Ball, Superplasticity in the Aluminium-Zinc Eutectoid—An Early Model Revisited, *Mater. Sci. Eng. A Struct. Mater. Prop. Microstruct. Process.*, 1997, **234**, p 365–369
12. T.G. Langdon, A Unified Approach to Grain-Boundary Sliding in Creep and Superplasticity, *Acta Metall. Mater.*, 1994, **42**, p 2437–2443
13. M. Ramos Azpeitia, E.E. Martinez Flores, and Villasenor G. Torres, Superplastic Behavior of Zn-Al Eutectoid alloy with 2% Cu, *J. Mater. Sci.*, 2012, **47**, p 6206–6212
14. R.A. Mitsuo, M.F. Elizabeth, N.S. Jesús, and G. Torres-Villaseñor, in *Characterization of Zinalco Alloy Superplastically Deformed Using Orientation Imaging Microscopy.* MRS Proceedings, (2011), p 1242
15. F.A. Mohamed and T.G. Langdon, Flow Localization and Neck Formation in a Superplastic Metal, *Acta Metall.*, 1981, **29**, p 911–920
16. M.K. Rao and A.K. Mukherjee, On the Evaluation of Parameters of the Constitutive Equation for 7475 Al-Alloy, *J. Mater. Sci.*, 1987, **22**, p 459–465
17. C.H. Caceres and D.S. Wilkinson, Superplastic Behavior of a Zn-22 pct Al-0.5 pct Cu Alloy, *Metall. Trans. A Phys. Metall. Mater. Sci.*, 1986, **17**, p 1873–1875
18. H. Naziri and R. Pearce, The Influence of Copper Additions on the Superplastic Forming Behaviour of the Zn-Al Eutectoid, *Int. J. Mech. Sci.*, 1970, **12**, p 513–521
19. T.G. Langdon, The Mechanical-Properties of Superplastic Materials, *Metall. Trans. A Phys. Metall. Mater. Sci.*, 1982, **13**, p 689–701
20. T.G. Nieh, J. Wadsworth, and O.D. Sherby, *Superplasticity in Metals and Ceramics*, Cambridge University Press, Cambridge, 1997
21. D.S. Wilkinson and C.H. Caceres, An Evaluation of Available Data for Strain-Enhanced Grain-Growth During Superplastic Flow, *J. Mater. Sci. Lett.*, 1984, **3**, p 395–399
22. M.G. Zelin, Processes of Microstructural Evolution During Superplastic Deformation, *Mater. Charact.*, 1996, **37**, p 311–329
23. B.P. Kashyap, A. Arieli, and A.K. Mukherjee, Microstructural aspects of Superplasticity, *J. Mater. Sci.*, 1985, **20**, p 2661–2686
24. L.C.A. Samuelsson, K.N. Melton, and J.W. Edington, Dislocation-Structures in a Superplastic Zn 40wt% Al-Alloy, *Acta Metall.*, 1976, **24**, p 1017–1026
25. O.A. Kaibyshev, S.N. Faizova, and A.F. Hairullina, Diffusional Mass Transfer and Superplastic Deformation, *Acta Mater.*, 2000, **48**, p 2093–2100
26. A.B. Ma, Y. Nishida, N. Saito, I. Shigematsu, and S.W. Lim, Movement of Alloying Elements in Mg-8 Center dot 5 wt-%Li and AZ91 Alloys During Tensile Tests for Superplasticity, *Mater. Sci. Technol.*, 2003, **19**, p 1642–1647
27. K.A. Padmanabhan, Grain Boundary Sliding Controlled Flow and Its Relevance to Superplasticity in Metals, Alloys, Ceramics and Intermetallics and Strain-Rate Dependent Flow in Nanostructured Materials, *J. Mater. Sci.*, 2009, **44**, p 2226–2238